 DOI: 10.1002/masy.201000036

Implementation of Specific Bioconjugation in Polystyrene-*block*-poly(*tert*-butyl acrylate)-Based Bio-Interfaces

*Ekram Wasse1, Sina Ghassemi, Holger Schönherr**

Summary: Here we report on the expansion of a previously introduced biointerface platform based on thin spin-coated films of polystyrene-*block*-poly(*tert*-butyl acrylate) (PS-*b*-PtBA). Following the selective deprotection of the *tert*-butyl-ester groups in the PtBA skin layer by hydrolysis under acidic conditions, the activation with *N*-hydroxysuccinimide and the subsequent derivatization with α,ω-biotin-amine end-functionalized poly(ethylene glycol) (PEG), strepavidin was immobilized as anchor layer for specific immobilization of biotin-tagged molecules. Based on contact angle, Fourier transform infrared (FTIR) spectroscopy, atomic force microscopy (AFM) and confocal fluorescence microscopy data it was shown that the polymer films were efficiently modified. The complexation of a biotin-tagged dye, as well as the non-specific adsorption of proteins was determined by confocal fluorescence microscopy measurements. The surface coverage of the immobilized dye as a function of dye concentration in solution was found to be consistent with a high affinity-type adsorption isotherm, while the protein resistant properties were found to be similar to non-biotinylated PEG. The scope of micro- and nanostructured PS-*b*-PtBA biointerfaces is thereby considerably expanded to encompass the specific immobilization of biotin-tagged biomolecules.

Keywords: biomaterials; diblock copolymers; polymer biointerfaces; thin films

Introduction

Structured and functionalized thin polymer films received increasing attention in recent years in the context of advanced materials and tailored interfaces for application in the areas of (bio)sensors and biologically oriented research involving biointerfaces.[1–3] In addition to compatibility with micro-/nanopatterning and -structuring methodologies[4–6] and the control of surface mechanical properties,[7–9] advanced biointerfaces require sophisticated surface chemistry to facilitate controllable bioconjugation and to implement the function of suppressing non-specific adsorption of proteins.[10] In view of the fundamental importance of an advanced understanding of cell-surface interactions in 2 and 3 dimensions,[11] but also for the fabrication of (bio)sensor surfaces, progress in this area is crucial for future applications in the biomedical field.

To address these needs, we previously introduced thin spin-coated films of polystyrene-*block*-poly(*tert*-butyl acrylate) (PS-*b*-P*t*BA) on various substrates as versatile, robust reactive platform for the immobilization of (bio)molecules for the fabrication of tailored biointerfaces.[12] The block copolymer incorporates three important functions, i.e. (*i*) a stabilizing glassy microphase of polystyrene to impart film stability and integrity under typical wet chemical processing conditions, (*ii*) a protected carboxylic acid functionality that can be conveniently deprotected to render high

Physical Chemistry, Universität Siegen, Adolf-Reichwein-Str. 2, 57076 Siegen, Germany
Fax: (+49) 271 740 -2805;
E-mail: schoenherr@chemie.uni-siegen.de

molecular loading via robust covalent (bio)conjugation feasible using active ester chemistry, and (*iii*) the implementation of chemical and topographic patterns on a broad range of length scales.[13,14] To this end the micro- and nanopatterning of the PS-*b*-P*t*BA via established and new soft lithographic approaches,[15,16] as well as the fabrication of 3-dimensional structures and films was investigated. In addition, the polymers films served as reactive platforms for various types of scanning probe nanolithography.[17]

Key to the function of biointerfaces is the optimized surface chemistry. To date we have demonstrated on PS-*b*-P*t*BA the successful covalent immobilization of amino-end functionalized DNA and poly(ethylene glycol) (PEG), proteins, including fibronectin, laminin, protein G and bovine serum albumin (BSA), as well as organic dyes etc.[12,13] This covalent conjugation is based on the selective deprotection of the *tert*-butyl-ester groups in the P*t*BA skin layer by hydrolysis under acidic conditions (Figure 1a) or by thermolysis, the activation with *N*-hydroxysuccinimide and the subsequent derivatization with amino functionalized (bio)molecules. The covalent coupling of proteins via pending amino groups leads to a robust attachment, however, this approach does not control the attachment point on the protein and may lead to multipoint attachment.

To overcome this problem of undefined protein conjugation on surfaces, specific molecular recognition has been exploited. The streptavidin/biotin system is of special interest in this context because of its large free energies of association.[18] In addition to this interaction pair, the interaction between Ni^{2+} and histidine tags has been exploited in this respect.[19–21] The noncovalent binding of a biotin to streptavidin in aqueous solution is characterized by a large equilibrium constant ($K = 10^{14}$ M^{-1}), which renders the immobilization practically irreversible. The complexes formed are also extremely stable over a wide range of temperature and pH. Since streptavidin possesses four binding pockets for biotin, biotin-tagged molecules can be conveniently immobilized on surface-attached streptavidin (Figure 1b).

In our current study the specificity of analyte binding of the PS-*b*-P*t*BA platform was significantly expanded by implementing the mentioned streptavidin - biotin complexation. By covalently grafting α,ω-biotin-amine end-functionalized PEG on activated PS-*b*-P*t*BA films the two necessary functions of specific streptavidin recognition and protein and cell repellence were combined. The immobilized streptavidin functions as a capture layer for arbitrary biotin-labeled (bio)molecules and thereby considerably expands scope of micro- and nanostructured PS-*b*-P*t*BA biointerfaces.

Experimental Part

Materials: PS_{2048}-*b*- P*t*BA_{1152} diblock copolymers (the subscripts refer to the number of repeat units of each block) were obtained from Polymer Source Company (Dorval, Canada) and were used as received (*total* $M_w = 387.75$ kg/mol, polydispersity index (PDI) = 1.10). Amino functionalized Biotin-PEG was purchased from Nektar U. K. Company ($M_n = 4847$ g/mol, PDI = 1.1). The biotinylated dye (Biotin – ATTO – 532) was purchased from ATTO – TEC – GmbH (Siegen, Germany).

Trifluoroacetic acid (TFA) and *N*-hydroxysuccinimide (NHS) were obtained from Sigma – Aldrich (Steinheim, Germany, purity ≥ 98%). *N*-(3-Dimethylaminopropyl)-*N*-ethylcarbodiimide hydrochloride (EDC) was purchased from Fluka (Steinheim, Germany, purity ≥98%). EDC was stored at −20 °C. Phosphate buffer saline (PBS) tablets were purchased from Sigma – Aldrich (Steinheim, Germany) to prepare phosphate buffer saline (pH 7.4, ionic strength = 0.1397 M). Silicon (100) wafers (P/Boron type) were applied as substrates. The cleaning of these substrates was done with piranha solution (solution of 1:3 (v/v) 30% H_2O_2 and concentrated H_2SO_4) for

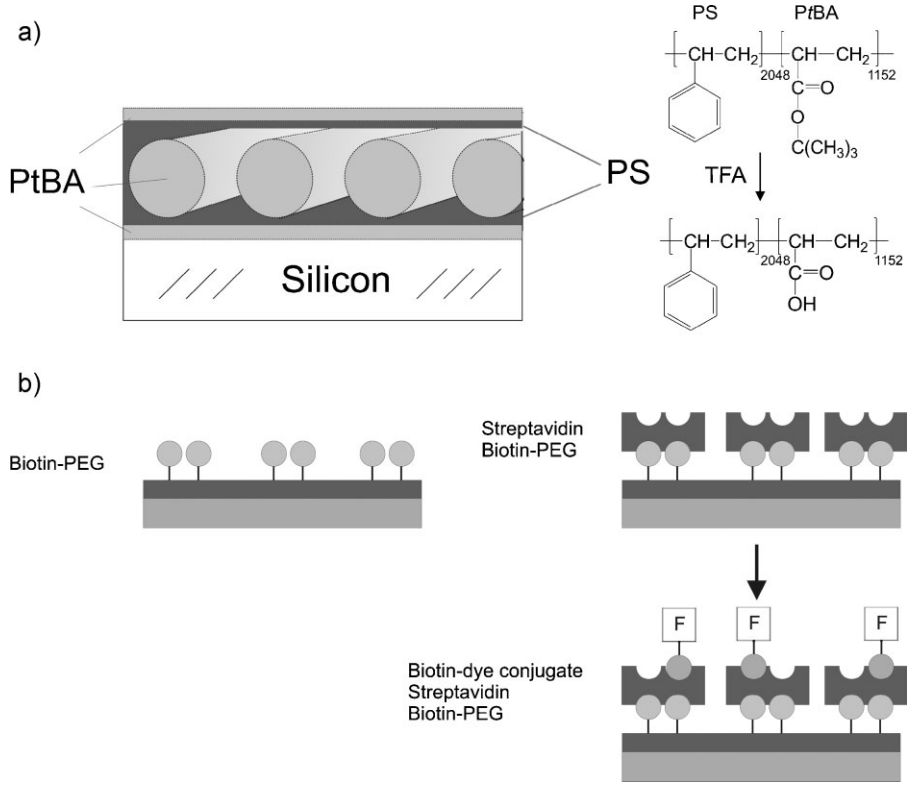

Figure 1.
(a) Schematic of film structure: Due to the lower interfacial free energies at both interfaces the PtBA phase shows symmetric wetting. Hydrolysis under acidic conditions converts the ester into carboxylic acid groups. (b) Grafting of biotin-PEG-NH_2 to hydrolyzed and NHS-activated PS_{2048}-*b*- $PtBA_{1152}$, specific binding of streptavidin to biotin-PEG, and high affinity binding of biotinylated fluorescence dye to streptavidin.

2 min and rinsed with copious amounts of high - purity water (E-Pure, Barnstead). Caution! Piranha solution should be handled with extreme caution; it has been reported to detonate unexpectedly.

Thin films were prepared by spin-coating polymer solutions in toluene (concentration 22.5 mg/mL) onto piranha – cleaned silicon wafers. The samples were spun at 3000 rpm for 60 s using a home-built spin-coater. All spin-coated films were annealed for 24 h at the temperature of 135 °C in vacuum before modification. The annealed polymer films were hydrolyzed at room temperature in neat TFA for 4 min, rinsed with high - purity water and finally dried in a stream of nitrogen. Then the films were activated by immersion in an aqueous solution of NHS (0.25 M) and EDC (0.20 M) for 60 min, followed by rinsing with PBS – solution (0.1379 M) and drying in a stream of nitrogen. The activated polymer films were immediately thereafter functionalized by immersion in an aqueous solution of biotin-PEG-NH_2 (1.0×10^{-4} M) for 60 min. After rinsing with high - purity water and drying in a stream of nitrogen, the films were modified by immersion in an aqueous solution of streptavidin (5.0×10^{-7} M) for 20 min. Then the films were rinsed with PBS - solution, dried in a stream of nitrogen and were modified by immersion in aqueous solutions of biotinylated dye (Biotin-Atto-532) with different concentrations (from 1.0×10^{-5} M to 2.0×10^{-10} M). Finally, the films were rinsed with high - purity water and dried in a stream of nitrogen.

Atomic Force Microscopy (AFM): The AFM images were taken in tapping mode with a NanoScope III multimode atomic force microscope (Digital Instruments/ Veeco) using Olympus tips (type OMCL-AC160TS, with a nominal cantilever elastic constant of 40 N/m) and a J- scanner in ambient atmosphere (20 °C).

Laser Scanning Confocal Microscopy (LSCM): The LSCM measurements were carried out on a home-built laser scanning confocal microscope in combination with a green Argon laser in fluorescence mode ($\lambda_{ex} = 532$ nm). The modified polymer films were investigated with an air-immersion objective lens with a numerical aperture of (0.75) and working distance of 210 μm. Fluorescence intensities were measured using a scan size of $10\,\mu m \times 10\,\mu m$ (100×100 pixels) at nine different positions on each sample.

Fourier Transform Infrared (FTIR) Spectroscopy: Transmission FTIR spectra (spectral resolution $4\,cm^{-1}$, 1000 scans) were obtained using an IFS 66V model FTIR spectrometer (Bruker) employing a liquid nitrogen-cooled cryogenic mercury cadmium telluride (MCT) detector. Background spectra were measured using piranha-cleaned silicon wafers.

Contact Angle (CA) Measurement: The static contact angles were measured after each step of reaction on a contact angle microscope (OCA 20, Data Physics) with high - purity water as probe liquid at room temperature.

Results and Discussion

The spin-coated diblock copolymer films, which comprise chemically distinct immiscible blocks of PS and P*t*BA, exhibited microphase separation in thin films on oxidized silicon. Intermittent contact mode AFM data showed wormlike structures (Figure 2a). From the power spectral density a typical repeat distance of 147 nm was determined. Upon annealing these films roughened considerably (Figure 2b). The rms roughness, evaluated on a scale of $5\,\mu m \times 5\,\mu m$, was found to increase from 0.8 nm for the non-annealed films to 2.8 nm after annealing.

The observed roughening can be tentatively attributed to a metastable or frustrated film morphology induced by the interplay of the interfacial energies. Wetting of the substrate with P*t*BA and exposition of the same block at the film-gas interface is favored, at the same time the film tries to adapt the cylindrical bulk morphology at this composition. Since we do not exploit the nanostructure of the block copolymer *per se*, the absence of long-range order on the nanoscale does not interfere with the intended application of the films. Important in the context of this

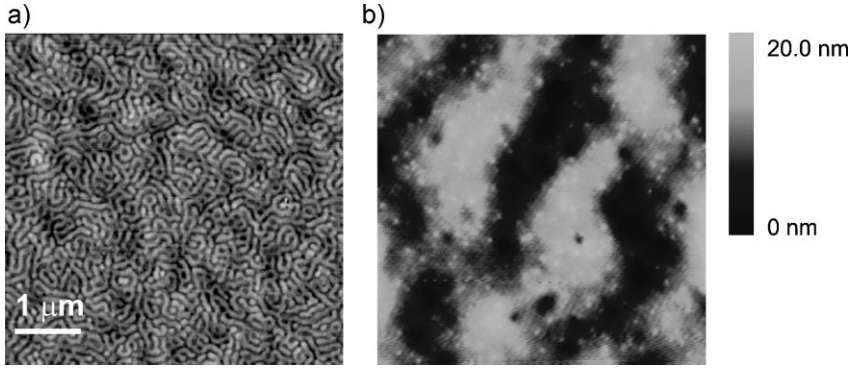

Figure 2.
Tapping mode AFM height images ($5\,\mu m \times 5\,\mu m$) of (a) as spin-coated and (b) annealed PS_{2048}-*b*- $PtBA_{1152}$ film (thickness 142 nm) on silicon.

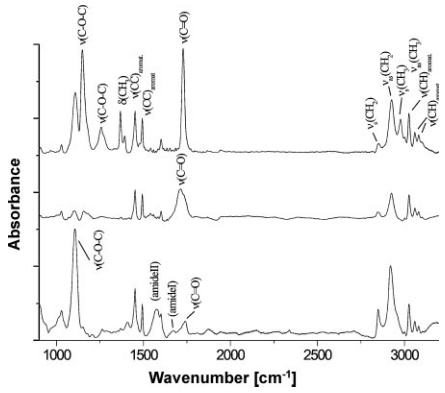

Figure 3.
FTIR spectra of a) spin-coated PS_{2048}-*b*- $PtBA_{1152}$, b) after hydrolysis of spin-coated film, c) after activation and coupling with biotin-PEG-NH_2.

report is the presence of a P*t*BA skin layer, which has been confirmed for various block copolymer compositions by X-Ray photoelectron spectroscopy (XPS),[22] and the stability of the films imparted by the water-insoluble PS block.

The successful hydrolysis and attachment of biotin-PEG was confirmed by contact angle measurements and in transmission FTIR measurements (Figure 3). The static contact angle measured with water as a probe liquid decreased upon hydrolysis from initially 87° to 40° - 60° (depending on the hydrolysis time); the PEG-biotin functionalized films showed contact angles between 15° and 30°.

The surface modification reactions were also analyzed by FTIR spectroscopy (Figure 3). Upon hydrolysis the C=O stretching vibrations were detected at lower wave numbers and the peak broadened considerably. In addition the absorbance of the peaks attributed to the deformation vibration of the methyl groups were greatly reduced in magnitude, indicating practically complete hydrolysis. The data are in line with previous reports. The C–O stretching vibrations of the ester were much less intense after hydrolysis. Consistently the band showed strong intensity after the coupling of the PEG. Finally, the amide I and II bands provide direct evidence for the covalent immobilization of the PEG derivative. The peak positions and full assignment is summarized in Table 1.

Subsequently, the block copolymer films were investigated before and after modification with the biotinylated dye with confocal fluorescence microscopy to quantify the background fluorescence and to monitor the intensity distributions as well as the lateral distribution of the immobilized dye. Figure 4a and 4c show fluores-

Table 1.
Assignment of bands observed in the FTIR spectra.

Vibration	PS block	PtBA block	PAA block	biotin-PEG-NH_2 layer
	cm^{-1}	cm^{-1}	cm^{-1}	cm^{-1}
ν $(CH)_{aromat.}$	3062			
	3052			
	3021			
$\nu_{as}(CH_3)$		2987		
$\nu_s(CH_3)$		2975		
$\nu_{as}(CH_2)$		2921		
$\nu_s(CH_2)$		2844		
ν(C=O)		1725	1712	1740
$\nu(CC)_{aromat.}$	1492			
	1450			
$\delta_s(CH_3)$		1367		
		1347		
ν(C–O–C)		1247		1106
		1147		
amide(I)				1671
amide(II)				1573

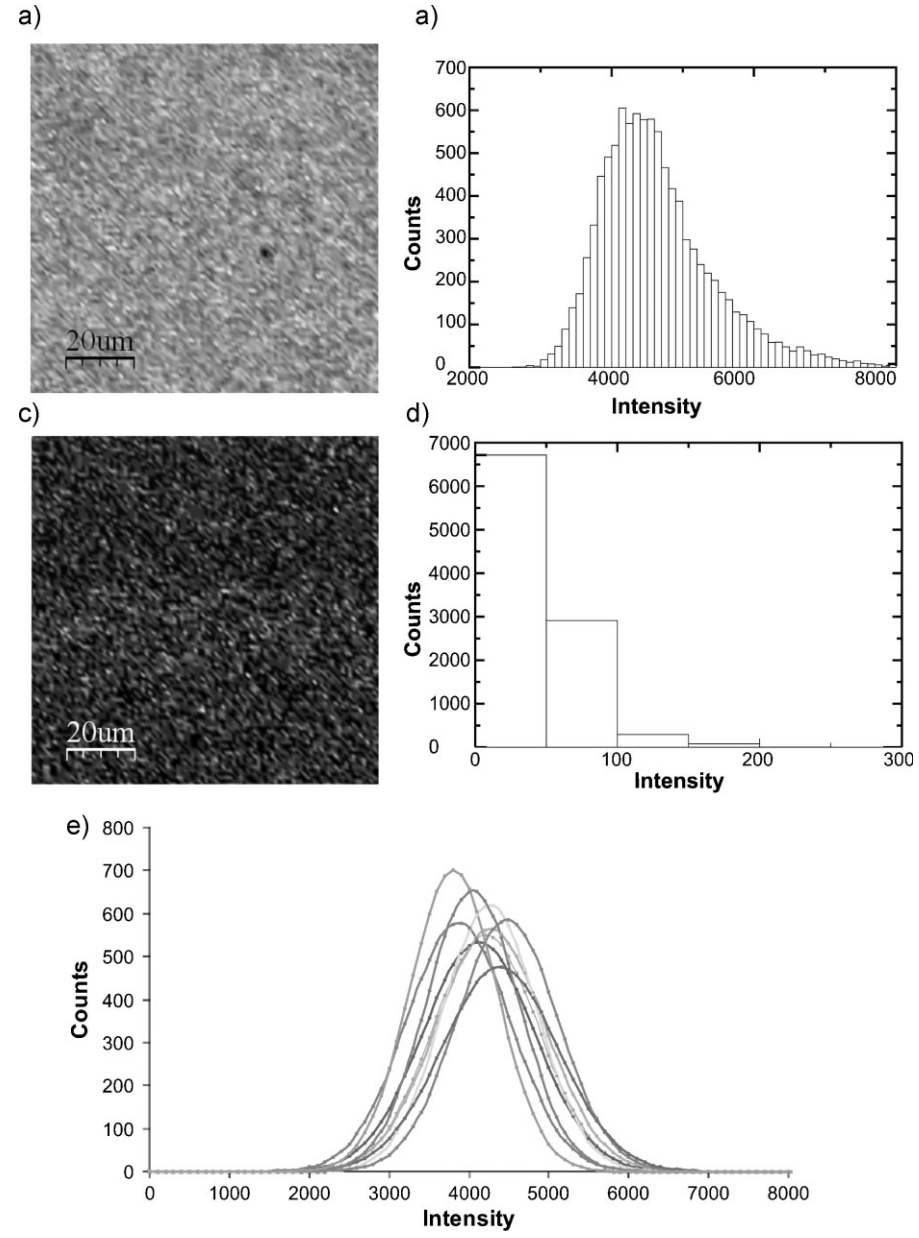

Figure 4.
(a,b) 100 μm × 100 μm CLSM images and corresponding intensity distributions of the biotinylated dye bound to streptavidin. The intensities in the two Figures cannot be directly compared since a different neutral density filter setting was used. (c,d) 100 μm × 100 μm CLSM image and corresponding distribution of a neat film of PS_{2048}-*b*- $PtBA_{1152}$. (e) 9 intensity distributions recorded at 9 different positions (10 μm × 10 μm) on the film.

cence microscopy images and Figure 4b and 4d the corresponding intensity distributions of the homogenous films, respectively. The high intensity of the biotinylated dye bound to the streptavidin-modified polymer films, as well we the very low background fluorescence of neat spin-coated polymeric film PS_{2048}-*b*- P*t*BA_{1152}

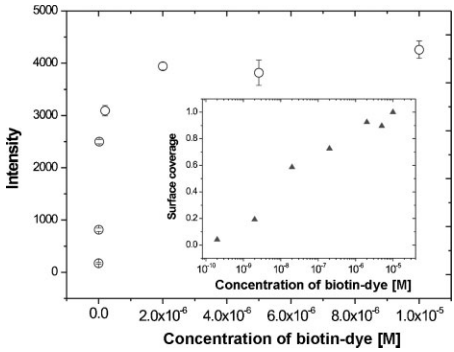

Figure 5.
Fluorescence intensity as a function of biotinylated dye concentration determined by confocal microscopy (inset: surface coverage).

are obvious. Hence these data imply that the biotin-streptavidin complexation afforded specific immobilization of the dye. This interpretation is further corroborated by an analysis of the concentration dependence of the dye loading on the film (dose response), as shown below in Figure 5. The lateral variations in dye loading were small, as indicated by the superposition of intensity distributions recorded at 9 different locations on a given film (Figure 4e).

The specific character of the biotin-mediated dye immobilization is evident from the relative coverage θ of the film with the dye (where $\theta = I/I_{max}$). As shown in Figure 5, an increase of the concentration of biotinylated dye in buffer resulted in an increase of θ. For concentration $> 2\,\mu M$ we observed a saturation in surface coverage (for an interaction time of 15 min.). The shape of this plot is consistent with a high affinity isotherm.

A comparison of the background fluorescence detected in the absence of the biotin-dye conjugate on the one hand and the measured fluorescence emission intensity for neat BCP films on the other hand shows that non-specific adsorption of the dye is negligible. The non-biotinylated PEG modified platforms have been previously shown to exhibit favorable non-specific adsorption properties when tested with bovine serum albumin, fibronectin or laminin.[12–14] Together with the specific biotin-streptavidin immobilization strategy implemented in this current work, the oriented and specific immobilization of biomolecules is now feasible on this polymer platform. This advanced surface chemistry will be combined with the possibilities of topographic structuring[14,16] for the investigation of cell-surface interactions in 3-D microwell arrays.

Conclusion

The thin film based biointerface platform of polystyrene-*block*-poly(*tert*-butyl acrylate) was derivatized with α,ω-biotin-amine end-functionalized poly(ethylene glycol) (PEG) using EDC/NHS chemistry. The subsequently immobilized streptavidin served as an anchor layer for specific immobilization of biotin-tagged molecules. The surface coverage of the immobilized dye as a function of dye concentration in solution was found to be consistent with a high affinity-type adsorption isotherm, while the protein resistant properties were found to be similar to non-biotinylated PEG. The scope of micro- and nanostructured PS-*b*-P*t*BA biointerfaces is thereby considerably expanded to encompass the specific immobilization of biotin-tagged biomolecules.

Acknowledgements: The authors thank Dr. Lars Birlenbach for technical support with the fluorescence microscope and Dr. Thomas Paululat for providing access to the FTIR spectrometer. Financial support of the University Siegen is gratefully acknowledged.

[1] R. Förch, H. Schönherr, A. T. A. Jenkins, Eds., *Surface Design: Applications in Bioscience and Nanotechnology*, Wiley-VCH, Weinheim 2009.
[2] D. G. Castner, B. D. Ratner, *Surf. Sci.* **2002**, *500*, 28.
[3] B. Kasemo, *Surf. Sci.* **2002**, *500*, 656.
[4] C. S. Chen, M. Mrksich, S. Huang, G. M. Whitesides, D. E. Ingber, *Science* **1997**, *276*, 1425.

[5] M. Arnold, E. A. Cavalcanti-Adam, R. Glass, J. Blummel, W. Eck, M. Kantlehner, H. Kessler, J. P. Spatz, *ChemPhysChem* **2004**, *5*, 383.
[6] D. Falconnet, G. Csucs, H. M. Grandin, M. Textor, *Biomaterials* **2006**, *27*, 3044.
[7] D. E. Discher, P. Janmey, Y. L. Wang, *Science* **2005**, *310*, 1139.
[8] D. E. Ingber, *J. Cell Sci.* **2003**, *116*, 1157.
[9] D. E. Ingber, *J. Cell Sci.* **2003**, *116*, 1397.
[10] G. L. Kenausis, J. Vörös, D. L. Elbert, N. P. Huang, R. Hofer, L. Ruiz-Taylor, M. Textor, J. A. Hubbell, N. D. Spencer, *J. Phys. Chem B.* **2000**, *104*, 3298.
[11] M. R. Dusseiller, D. Schlaepfer, M. Koch, R. Kroschewski, M. Textor, *Biomaterials* **2005**, *26*, 5917.
[12] C. L. Feng, A. Embrechts, I. Bredebusch, A. Bouma, J. Schnekenburger, M. García-Parajo, W. Domschke, G. J. Vancso, H. Schönherr, *Eur. Polym. J.* **2007**, *43*, 2177.
[13] C. L. Feng, A. Embrechts, I. Bredebusch, J. Schnekenburger, W. Domschke, G. J. Vancso, H. Schönherr, *Adv. Mater.* **2007**, *19*, 286.
[14] A. Embrechts, C. L. Feng, C. Mills, M. Lee, I. Bredebusch, J. Schnekenburger, W. Domschke, G. J. Vancso, H. Schönherr, *Langmuir* **2008**, *24*, 8841.
[15] C. L. Feng, G. J. Vancso, H. Schönherr, *Langmuir* **2007**, *23*, 1131.
[16] J. Duvigneau, S. Cornelissen, N. Bardají Valls, H. Schönherr, G. J. Vancso, *Adv. Funct. Mater.* **2010**, *20*, 460.
[17] J. Duvigneau, H. Schönherr, G. J. Vancso, *Langmuir* **2008**, *24*, 10825.
[18] M. Wilchek, E. Bayer, *Avidin-Biotin Technology Methods in Enzymology*, Academic Press, San Diego 1990, 184.
[19] F. H. Arnold, *Metal-Affinity Protein Separations*, Academic Press, San Diego 1992.[(b)] E. Hochuli, *Genet. Eng.* **1990**, *12*, 87.
[20] E. Hochuli, W. Bannwarth, H. Dçbeli, R. Gentz, D. Stuber, *Bio-Techniques* **1988**, *6*, 1321.
[21] G. Zhen, D. Falconnet, E. Kuennemann, J. Vörös, N. D. Spencer, M. Textor, S. Zürcher, *Adv. Funct. Mater.* **2006**, *16*, 243.
[22] C. L. Feng, G. J. Vancso, H. Schönherr, *Langmuir* **2005**, *21*, 2356.

